Theoretical Analysis of Microscopic Forces at Soil-tool Interfaces: A Review

Peeyush Soni[1] Vilas M. Salokhe[1]

[1]Agricultural Systems and Engineering
Asian Institute of Technology
P.O. Box 4, Klong Luang
Bangkok, Thailand
salokhe@ait.ac.th

ABSTRACT

Soil-tool interaction has been a prime concern of research about soil-engaging tools used both in agricultural and construction machinery. Forces acting on a soil-engaging tool can be broadly understood by classifying them into two groups – macroscopic, the forces extensively depend on the system parameters including tool type, tool speed, soil properties, and operating depth; and microscopic – largely rely on intrinsic properties of tool surface, soil composition, physical and chemical properties of soil and molecular phenomena. Practical difficulty and complicacy experienced by researchers in demarcating adhesive and frictional forces at the soil-tool interface led a newer approach of grouping such forces into mutually perpendicular components – normal (N) and tangent (τ) at the interface for determining total microscopic force (F). Normal force acting at the interface comprises three primary components – normal gravity, normal adhesion and normal friction, whereas tangent resistance constitutes three components – tangential friction, drag and tangential adhesion. This paper theoretically analyzes microscopic forces at the soil-tool interface and hence opens a window to further evaluate these concepts for various soil types with different tool shapes.

Keywords: Microscopic interfacial forces, adhesion, viscosity, friction, capillary adsorption, surface tension, soil-engaging tools, soil-tool interface

1. INTRODUCTION

There are various mechanisms through which two particles in the nature exert force on each other; the force of attraction between them is a usual natural phenomenon. Depending on the particle type it can be cohesion – if the two particles are from the same parent material, or can be adhesion – if the two come from different parent material. Cohesion and adhesion are the molecular phenomenon occurring at the interface of a liquid and gas, result from electrical interactions of the solid microscopic particles. The maximum distance up to which the force of cohesion between molecules can act is known as their *molecular-range* ($\approx 10^{-7}$ cm) (Oswal, 1994). An imaginary sphere drawn around a molecule with its radius equal to the molecular range and center coinciding center of the molecule is called the *sphere of influence* of the molecule.

P. Soni and V. Salokhe. "Theoretical Analysis of Microscopic Forces at Soil-tool Interfaces: A Review". Agricultural Engineering International: the CIGR Ejournal. Manuscript PM 06 010. Vol. VIII. June, 2006.

May it be farm implements, construction machinery or any soil-engaging tool, their larger force requirement increases the input energy and hence lesser work is resulted per unit effort supplied, which is especially significant in sticky soils. In agricultural applications, soil-tool adhesion is of greater importance – especially when prevailing soil is rich in clay content and hence sticky by nature. Various investigations have been carried out to study adhesion mechanism, to quantify soil-adhesion properties, to determine their contributing factors, and for developing means of reducing soil-adhesion (Gill and Vanden Berg, 1968; Chancellor, 1994; Ren et al., 2001).

Earlier researches on tangent resistance have clearly indicated that it is composed of the frictional and adhesive – two components (Shi-qiao, 2004). Forces acting on a soil-engaging tool can be broadly understood by classifying them into two groups – macroscopic, the forces extensively depend on the system parameters including tool type, tool speed, soil properties, and operating depth; and microscopic – largely rely on intrinsic properties of tool surface, soil composition, physical and chemical properties of soil and molecular phenomena. Oida and Momozu (2002) used distinct element method (DEM) to analyze soil forces and found that it was successful from both the soil behavior and reaction points of view.

As per the definition of adhesion, soil-engaging tool and soil particles are the two rigid bodies with unlike material properties, where an additional force, acting on their mutual contact surface, is often required to pull them apart. This additional force of attraction, depending on various factors, often attains noticeable magnitude and has been inviting special attention for decades. Soil adhesion decreases quality of work, reduces efficiency of soil-tool, and increases energy consumption per unit soil operation. Studies reveal a reduction of as high as 30–50% in the work efficiency of soil-engaging components of earth moving and construction equipment, which include dumpers, bulldozers, and excavators; whereas soil adhesion is assumed to contribute to rolling resistance of soft-ground vehicles on paddy fields, swamps and beaches (Ren et al., 2001).

Practical difficulty and natural complicacy to clearly demarcate the adhesive and frictional components (Shi-qiao, 2004) of total microscopic forces needs a simultaneous approach of analysis. Based on various theories previously suggested, the present description attempts to classify such microscopic forces at soil-tool interface into normal forces and tangential resistance and consequently elaborates their individual nature and constituents.

Fountaine (1954), Qian (1965), Akiyama and Yokoi (1972), Cong et al. (1990) and Shi-qiao (2004) proposed mechanical models to analyze soil resistance at soil-tool interface. Such models assume cutting of soil by a planer tool surface, which could reasonably represent the actual mechanism (Shi-qiao, 2004).

A greater maneuverability can be achieved upon knowing microscopic forces at soil-tool interface to reduce draft requirement by lowering various components contributing to the total interfacial force. Microscopic forces are both important and necessary to be addressed (Israelachvili et al., 1982) while designing a soil-engaging tool, especially in soils with high clay content. Many researchers have proposed different models to analyze such forces with particular emphasis on normal adhesion (Jia, 2004), tangential adhesion (Akiyama and Yokoi, 1972; Shi-qiao, 2004), chemical adsorption (Chen et al., 1996), friction (Liu, 1993), capillary attraction (Bikerman, 1974; McFarlance and Tabor, 1950; Orr and Scriven, 1975) and liquid bridge force (Zhang et al., 2004a; 2004b; 2006). The present study combines

intermolecular, gravitational, adhesive, capillary, frictional and viscous forces occurring at the planer soil-tool interface. A theoretical model is proposed after reviewing existing principles and grouped under two mutually perpendicular components viz. normal and tangent to the interface.

In this analysis, following assumptions were used:

a) To avoid the complexity of analysis, the interface is assumed to be a planer surface.
b) The total gravitational stress at the interface is mainly due to soil particles and water-filled soil pores. The maximum gravitational force can be calculated when all soil pores are filled with water, since voids have no contribution to it.
c) Soil particles are spherical, smooth and identical. Deformation at the interface is neglected. For the simplicity in computation, soil particles are assumed to be un-clustered.
d) Tool surface is smooth and free from micro-irregularity.
e) Contact angle of water on soil is zero.
f) Surface tension of water remains constant, irrespective of temperature change.

2. NORMAL FORCES ACTING AT SOIL-TOOL INTERFACE

Normal forces (N) acting at the interface have three components, viz. normal gravity, normal adhesion and normal wet friction.

2.1 Normal Gravitational Force (N_G)

Contact area at the soil-tool interface is a key parameter affecting normal forces at the tool surface. A representative soil sample can be cut by a thin steel wire (Tong et al., 1994) to examine spatial constitution of soil particles and pores. A unit cross section at the soil-tool interface can be considered, where soil pores randomly occupy *p%* of total cross sectional area at the interface. Thus only (1–*p*) fraction of area falls under direct soil-tool contact.

If S_i is the area of individual soil pore, the total porous area at the interface will be summation of all such pores. It should be noted that these randomly distributed pores may be having different individual dimensions. Thus the total porous area at the interface S_p,

$$S_p = \sum S_i \qquad \text{... (1)}$$

The total porous area S_p and the total area of soil-tool contact at the interface (S_s) can be related to the interfacial cross sectional area (S) as,

$$S_p = p.S \qquad \text{... (2)}$$

$$S_s = (1-p).S \qquad \text{... (3)}$$

Where,

$$S = S_p + S_s \qquad \text{... (4)}$$

The maximum gravitational force, acting normally downward at the interface can be expected when all the soil pores are filled with water. If σ_p is the mean gravitational stress of soil pores, σ_s is the mean gravitational stress of soil particles then the total gravitational force at interface N_G, can be given as,

$$N_G = N_p + N_s \quad \text{... (5)}$$

Where,

N_p = Weight of water-filled soil pores
N_s = Weight of soil particles

Or,

$$N_G = \sigma_p.S_p + \sigma_s.S_s \quad \text{... (6)}$$

Gravitational force of soil particles also contributes to the frictional component of normal forces, whereas water-filled soil pores play role in adhesive component of normal forces. Substituting values of S_p and S_s from Eqns. (2 & 3), Eqn. (6) can be reduced for total interface area (S) as,

$$N_G = \sigma_p.p.S + \sigma_s.(1–p).S \quad \text{... (7)}$$

$$N_G = \sigma_s.S – (\sigma_s – \sigma_p).p.S \quad \text{... (8)}$$

2.2 Normal Adhesive Force (N_A)

Normal adhesive force at the soil-tool interface depends on various factors including soil properties, tool material, tool surface, soil water content and interfacial conditions. Zeng (1995) claimed that the soil adhesion to soil-engaging tool increased with normal stress on it. The normal adhesion can be treated as having action similar to that of normal load at the interface (Fountaine, 1954; Gill and Vanden Berg, 1968).

Soil water content variation, at micro level, causes significant alteration in status of soil particles and its respective interface with tool surface. Jia (2004) revealed a direct relationship of soil adhesive force with the interface situation between soil and tool surface. Zeng (1995) and Shi-qiao (2004) described such interfaces at four water content levels, which are summarized in Table 1.

Various possible contact models of soil particles on tool surface at different water content stages are shown in Figure 1. Dry friction dominants between soil particles and tool surface for the oven dried bare soil particles and particles enveloped by closely confined water. With increase in water content up to a certain limit, viscous forces and wet friction also become significant.

For some physically isolated soil particles an oven dried bare condition can be assumed, where theoretically zero water content attributes to the maximum water adsorptive tendency (Figure 1a). Depending on the system parameters, such particles rapidly get converted into other water stages. Friction generated from the rubbing and scratching action of dry soil particles on tool surface (Liu, 1993) is the major contributor to interfacial forces, while the

viscous, adsorptive and adhesive forces might be neglected for this water stage (Shi-qiao, 2004).

Table 1. Status of soil particle and soil-tool interface with soil water variation

	Soil water content range	Status of soil particle	Soil-tool interface	Water status at interface	Contribution to interfacial forces
a)	Zero – Max water adsorption content	Oven dried bare particle	Bare soil particle-tool interface	No water	▪ Dry friction ▪ Small adhesion
b)	Max water adsorption content – Max molecular holding water content	Enveloped by closely confined film-like water	Closely confined water enveloped soil particle-tool interface	Film-like water	▪ Physico-chemical adsorption of soil particles
c)	Max molecular holding water content – Field holding water content	Enveloped by water film	Water film enveloped soil particle-tool interface	Water film produced by film-like water	▪ Physico-chemical adsorption of soil particles ▪ Capillary negative adsorption ▪ Meniscus adhesion
d)	Capillary water – Saturated water content	Enveloped by gravitational water	Gravitational water enveloped soil particle-tool interface		▪ Meniscus tension ▪ Viscidity ▪ Wet friction ▪ Imperfect capillary adsorption

In the process of adsorption, at the water content between maximum water adsorption to maximum molecular holding (Figure 1b) bare particle is bounded with only a few water molecule thick water layer ($\approx 10^{-7}$ cm) (Oswal, 1994; Xiong, 2001; Zeng, 1995), supported by Hydrogen bonds. Strong intermolecular force between soil and closely confined water molecules neither facilitate viscidity nor dissolving. No water film is formed at the soil-tool interface. Behavior of this stage can be characterized intermediate between it's former and latter water stages.

A further increase in water content brings soil particles at the interface under envelope of water film of 10–20 water molecule thickness ($\approx 10^{-6}$ cm) (Shi-qiao, 2004). Physico-chemical adsorption is the main contributing factor at this water content stage (Figure 1c). The intensity of physico-chemical adsorption greatly depends on soil composition. For soils with high clay content, about 30% of total soil water is in the form of water film, whereas it is 15% in loamy soils and only 1.5% in sandy soil and (Shi-qiao, 2004).

Increasing water content introduces gravitational water, allowing capillary rise and meniscus formation. Meniscus tension, viscous force and wet friction are summing up to total interfacial forces at this water content stage (Figure 1d).

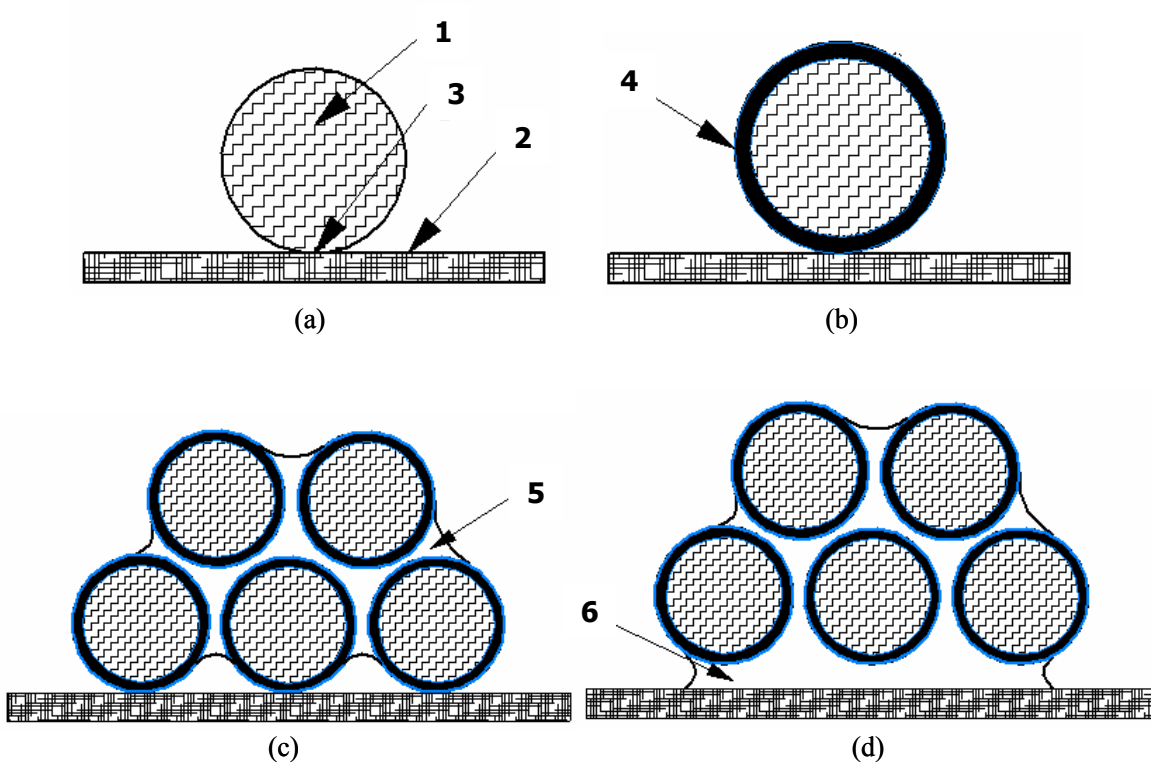

Figure 1. Various possible contact models of soil particles on tool surface at different water stages: (a) adsorption water; (b) molecular water; (c) field holding water and (d) gravitational water; 1- soil particle; 2- tool surface; 3- soil-tool interface; 4- closely confined water; 5- water meniscus and 6- gravitational water (figure not to scale)

Ren et al. (2001) described surface morphologies of soil at contact interfaces. They reported that roughness of soil surfaces, formed at the contact interface could be found in three sizes, micro-aggregate, particle, and asperity on particles. The soil particles, for avoiding complexity, could be assumed to be smooth and spherical (Jia, 2004). Soil water content directly governs interfacial contact condition. As a broad classification there can be soil-tool contact with or without water ring. Again, status of water ring at the interface differs with soil water. With high water content or at higher normal loads, the interface is filled with water and a continuous film links soil to tool surface. In contrast, with low water contents or at lower normal loads, a non-continuous water film exists. Based on the surface morphology and soil water status at the contact interface, five soil-tool contact models, as depicted in Figure 2, could be defined (Ren et al., 2001; Tong et al., 1994; Jia, 2004).

a) Completely non-contacting asperity without water ring
b) Water-point contacting asperity without water ring
c) Water-ring contacting asperity
d) Water-loop contacting asperity
e) Continuous water film

The normal adhesion force at the interface comes from forces mainly caused by intermolecular attraction of bare soil particles (N_{As}), attraction of water meniscus (N_{Am}), attraction of water film due to viscosity (N_{Av}) and capillary negative adsorption (N_{ca}).

2.2.1 Normal Adhesion Caused by Intermolecular Attraction of Bare Soil Particles (N_{As})

Considering the contact models where situation states absence of water between soil particle and tool surface (Figure 2(a&b)), intermolecular attraction is caused by molecular interaction between them.

For a non-contacting (Figure 2a) spherical asperity (radius R), attraction pressure per unit area of separation (unit area of separation is defined as the separation of the tip of the summit to the tool surface) *P(d)*, can be expressed as a function of its separation (d) between asperity summit and the solid surface using Lennard-Jones function (Tong et al., 1994),

$$P(d) = \frac{\partial E(d)}{\partial d} \qquad \ldots (9)$$

where *E(d)* is interaction energy per unit area of separation. The interaction energy will be the energy of adhesion (E_A) at the equilibrium intermolecular distance d_e (Tong et al., 1994),

$$P(d) = \left(\frac{8E_A}{3d_e}\right)\left[\left(\frac{d_e}{d}\right)^3 - \left(\frac{d_e}{d}\right)^9\right]; \; E(d_e) = E_A \text{ at } d = d_e \qquad \ldots (10)$$

The interaction energy per unit area of separation between two parallel planes, as a function of *d*, was defined by Lifishitz's theory (Wu, 1982),

$$E(d) = \frac{h\omega}{16\pi^2 d^2} \qquad \ldots (11)$$

Where,

$h\omega$ = Lifishitz-Van der Waals constant

At the separation equal to intermolecular distance, $E(d_e)$ gives the work of adhesion (Jia, 2004),

$$W_A = E(d_e) = E_A = \frac{h\omega}{16\pi^2 d_e^2} \qquad \ldots (12)$$

where E_A was expressed as (Jia, 2004),

$$E_A = \frac{h\omega}{8\pi}\left[\frac{R}{d_0} - \ln\left(\frac{d_0 + R}{d_0}\right)\right] \qquad \ldots (13)$$

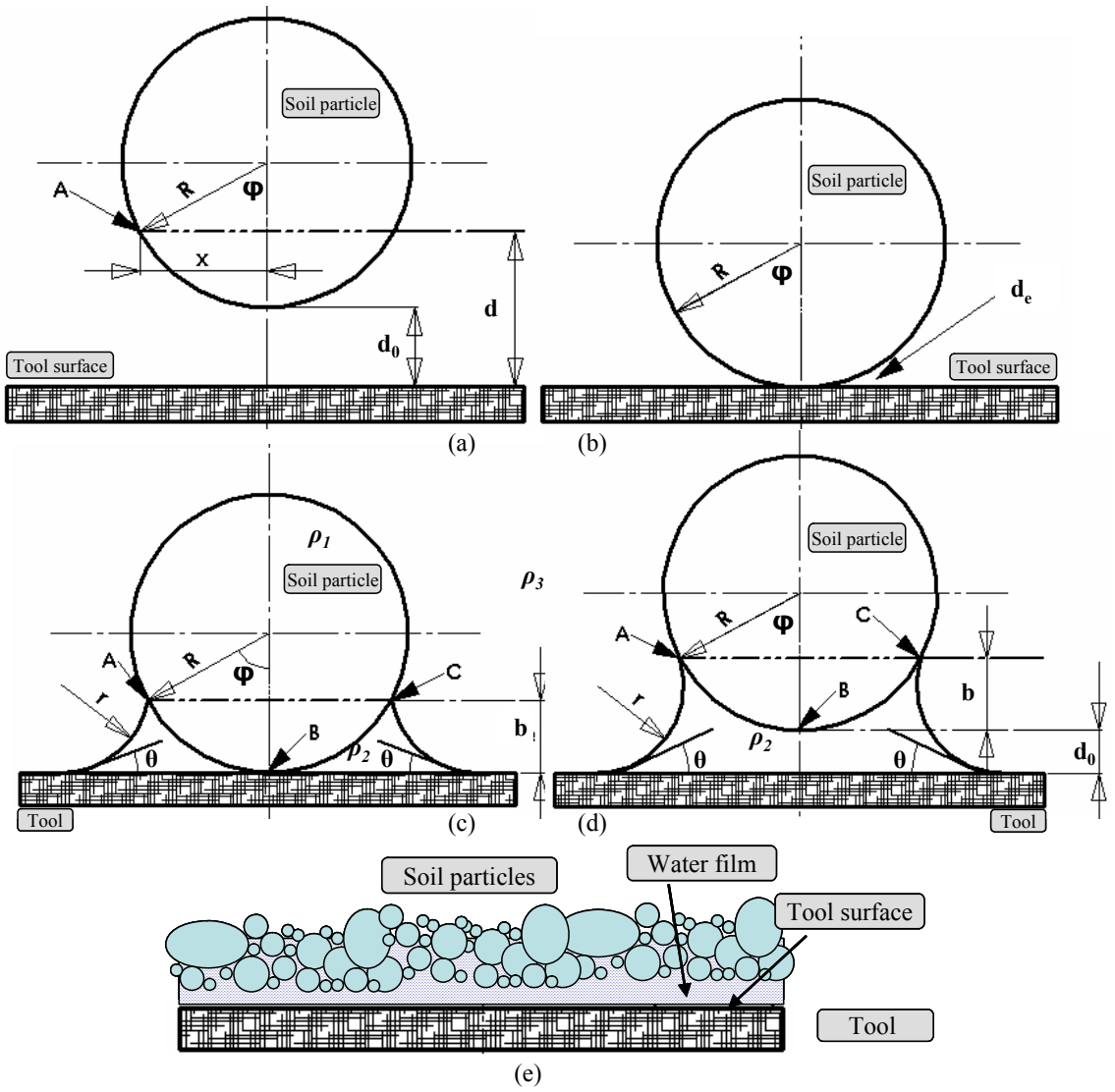

Figure 2. Contact models of soil-tool interface: a) completely non-contacting asperity without water ring; b) water-point contacting asperity without water ring; c) water-ring contacting asperity; d) water-loop contacting asperity and e) continuous water film (figure not to scale) (modified and redrawn after Jia, 2004)

The normal adhesion caused by intermolecular attraction force of bare soil particles (N_{As}) was expressed by Jia (2004),

$$N_{As} = \frac{-\partial E_A}{\partial d_0} = \frac{-h\omega}{8\pi}\left[\frac{R}{d_0^2} - \frac{R}{d_0(d_0+R)}\right] \quad \ldots (14)$$

Where,

d_0 = Separation between the summit tip and tool surface

Negative sign in Eqn. (14) shows that N_{As} is of attraction characteristics, i.e. if tool is assumed stationary then soil is attracted towards the tool surface.

From Eqns. (12 & 14), magnitude of N_{As} (Jia, 2004),

$$N_{As} = 2\pi.W_A d_e^2 R.\left[\frac{1}{d_0^2} - \frac{1}{d_0(d_0+R)}\right] \quad \ldots (15)$$

For a water-point contacting asperity without water ring ($d_0 = d_e$), the magnitude of normal adhesion due to intermolecular interaction can be expressed by simplifying Eqn. (15) as (Jia, 2004),

$$N_{As} = 2\pi.W_A R.\left[1 - \frac{d_e}{(d_e+R)}\right] \text{ at } (d_0 = d_e) \quad \ldots (16)$$

Alternatively, if Lifishitz-Van der Waals constant is unknown or difficult to calculate, Eqn. (15) can be expressed in terms of E_A (Tong et al., 1994),

$$N_{As} = \frac{8}{3}\pi.R.E_A\left[\left(\frac{d_e}{d_0}\right)^2 - \frac{1}{4}\left(\frac{d_e}{d_0}\right)^8\right] \quad \ldots (17)$$

In Eqn. (17), for a reasonable approximation, if no water molecule is absorbed at the surface of soil particle, then E_A can be expressed as the work of adhesion (W_A) (Tong et al., 1994),

$$E_A = W_A = \gamma_{SV} + \gamma_{LV} - \gamma_{SL} \quad \ldots (18)$$

Where,

γ_{LV} = Surface tension at liquid-vapor interface
γ_{SL} = Surface tension at solid-liquid interface
γ_{SV} = Surface tension at solid-vapor interface

But the surface of soil particle normally absorbs at least a layer of water molecules then E_A will be expressed as (Tong et al., 1994),

$$E_A = 2\,\gamma_{LV} \quad \ldots (19)$$

2.2.2 Normal Adhesion Caused by Water Meniscus (N_{Am})

When the water film becomes thicker, gravity water also joins the interfacial film, and normal adhesion is produced by the meniscus adjacent to soil particle (Shi-qiao, 2004). Water ring formed between the soil particle and planer tool surface (Figure 2(c&d)) results in meniscus tensile force, acting in the direction of surface tension i.e. tangent at the meniscus-tool contact. Assuming the contact angle of water on soil particle as zero, θ be the contact angle between meniscus and tool surface, Jia (2004) suggested an expression for magnitude of adhesion force (F_{Am}), in the direction of surface tension,

$$F_{Am} = \frac{2\pi.R.\gamma}{\left[1+\frac{d_0}{b}\right]}(1+Cos\theta) \qquad \ldots (20)$$

Where,

F_{Am} = Adhesion force of water meniscus, in the direction of surface tension
b = Vertical distance between soil particle surface to its lowest tip

Vertical component of Eqn. (20) will give magnitude of the normal adhesion caused by water meniscus (N_{Am}),

$$N_{Am} = F_{Am}.Sin\ \theta = \frac{2\pi.R.\gamma}{\left[1+\frac{d_0}{b}\right]}(1+Cos\theta).\ Sin\ \theta \qquad \ldots (21)$$

Consequently, Princen (1969) explained that the ring shaped liquid wedge (density ρ_2), between a solid spherical particle (radius R, density ρ_1) and a horizontal tool surface cause the downward force to increase by the amount, which is the normal adhesive force (N_{Am}),

$$N_{Am} = 2\pi\ R\ \gamma\ Sin^2\ \varphi - \frac{\pi}{3}\ (\rho_2 - \rho_3).g\ R^3\ (1 - Cos\ \varphi)^2\ (2 + Cos\ \varphi)$$
$$- (\pi\ R^2\ Sin^2\ \varphi\ .P_{AC}) \qquad \ldots (22)$$

Where,

N_{Am} = Normal adhesion caused by water meniscus
ρ_3 = Density of second fluid surrounding the whole system
φ = Angle, with vertical, made by the radius with the point at which the liquid surface meets sphere
P_{AC} = Negative pressure existing at the liquid wedge at the level AC

The first (positive) term in Eqn. (22) represents the downward component due to surface tension; the second (negative) term represents the upward force experienced by the volume ABC, which is submerged in liquid; and the third (negative) term represents the upward force resulted from the *negative pressure* P_{AC} existing in the liquid wedge at level AC, relative to the pressure in the third fluid (density ρ_3) at the same level (Princen, 1969),

$$P_{AC} = \frac{-\gamma}{R_{AC}} \qquad \ldots (23)$$

Where,

R_{AC}= Radius of curvature of the interface at point A

For small values of R and φ, and zero contact angles, circular profiles are obtained. Thus, in such cases, the radius of this circular meniscus (r) is given as (Princen, 1969),

$$r = \frac{(1-Cos\ \varphi)}{(1+Cos\varphi)}.R \qquad \ldots (24)$$

and the negative pressure in the wedge, relative to the outside can be given as (Princen, 1969),

$$P - P_0 = P_{AC} = -\frac{\gamma}{r} \quad \ldots (25)$$

$$P_{AC} = -\left(\frac{\gamma}{R}\right)\frac{(1+Cos\,\varphi)}{(1-Cos\,\varphi)} \quad \ldots (26)$$

Substituting the values of r and P_{AC} in the Eqn. (22), and neglecting the second term for small values of φ we get,

$$N_{Am} = \pi R \gamma (1 + Cos\,\varphi)(3 - Cos\,\varphi) \quad \ldots (27)$$

The normal adhesive force (N_{Am}), between the soil particle and plate can be computed as per the concept of capillary rise, which states that the force of adhesion will be equal to the contact perimeter (2 * 2πR), surface tension (γ) and the cosine of the contact angle (θ) (Gill & Vanden Berg, 1968).

Thus,

$$N_{Am} = 4\pi R \gamma\, Cos\,\theta \quad \ldots (28)$$

The maximum normal adhesive force obtained (Israelachvili et al., 1982; Jia, 2004; McFarlance and Tabor, 1950; Princen, 1969) would be,

$$(N_{Am})_{max} = 4\pi R \gamma \quad \ldots (29)$$

2.2.3 Normal Adhesion Caused by Attraction of Water Film Due to Viscosity (N_{Av})

Viscosity is the property that opposes relative motion between two layers of liquid (Oswal, 1994) and it can be understood as the internal friction of the liquid that brings resistance to flow (Michael, 1998). Gill and Vanden Berg (1968) revealed that viscosity and loading rate affect the adhesion. For the contact model with water film between two parallel solid planes (Figure 2e) an analogy of two circular discs of radius R, immersed in a liquid of viscosity η could be applied (Jia, 2004). If they are subjected to a tensile force (N_{Av}) their separation increases from h_1 to h_2, just before the liquid film does not break during pull. If the time required to pull is t, the N_{Av} can be expressed (Bikerman, 1970; Bowden and Tabor, 1954; Ren et al., 2001) as,

$$N_{Av} = \left(\frac{3\pi.\eta.R^4}{4t}\right)\left(\frac{1}{h_1^2} - \frac{1}{h_2^2}\right) \quad \ldots (30)$$

2.2.4 Normal Adhesion Due to Capillary Negative Adsorption (N_{ca})

Soil porosity contributes an important role to adhesive forces. These pores are either filled with air or water. Xiong (2001) classified soil pores into three categories namely inactive pores (equivalent diameter <2 μm), capillary pores (equivalent diameter 2 – 20 μm) and air pores (equivalent diameter >2 μm). The soil particles interact with soil water through either physico-chemical or physico-mechanical process. The friction and adhesion of air can be neglected whereas inactive pores contribute little either. The adhesion between capillary pores and tool surface is noticeable and is mainly due to the capillary adsorption.

Upon immersing the tube (radius R_c) in a liquid (density ρ), the capillary rise of liquid will take place due to surface tension of liquid (γ) and a meniscus will form corresponding to the contact angle (θ) of liquid on the tube material. The height of capillary rise (h) can be determined at its equilibrium condition, where upward force caused by surface tension would balance weight of the lifted liquid column,

$$2 \pi R_c \gamma Cos \theta = \pi R_c^2 \rho g h \quad \ldots (31)$$

$$h = \frac{2\gamma Cos\theta}{\rho g R_c} \quad \ldots (32)$$

a pressure difference (ΔP) exists at the two surfaces of meniscus, which causes capillary ascent, is expressed by Young-Laplace equation, at static condition (Figure 3a),

$$\Delta P = P - P_0 = \frac{2\gamma . Cos\theta}{R_c} \quad \ldots (33)$$

Where,

P = Pressure inside liquid column near the meniscus

P_0 = Atmospheric pressure

When a tool acts on soil mass, the process can be regarded as shearing of soil capillaries at the interface (Shi-qiao, 2004). Shi-qiao et al. (2005) described the mechanism of capillary snipping in their snipping-capillary test. To understand the process, a section of ascending sheared capillary (Figure 3b) can be considered having two meniscus – upper and lower. Applying Young-Laplace equation to calculate pressure difference at upper meniscus (ΔP_1) and at lower meniscus (ΔP_2), we get,

$$\Delta P_1 = P_1 - P_0 = \frac{-2\gamma . Cos\theta_1}{R_c} \quad \ldots (34)$$

$$\Delta P_2 = P_2 - P_0 = \frac{-2\gamma . Cos\theta_2}{R_c} \quad \ldots (35)$$

where P_1 and P_2 are pressures inside the liquid near the upper and lower meniscus, respectively and θ_1 and θ_2 are contact angles of liquid with tube at upper and lower meniscus respectively. For an ascending capillary, ΔP_1 and ΔP_2 should obviously be negative.

At any instant, the net ascending pressure difference for the liquid segment, should balance the static pressure of lifted liquid column (P_{static}) that is the weight of liquid column segment. Thus, for the instantaneous partial equilibrium,

$$\Delta P_1 - \Delta P_2 = P_{static} \quad \ldots (36)$$

If s is the distance between the lowest point of upper meniscus and the shearing plane,

$$[\frac{-2\gamma.Cos\theta_1}{R_c}] - [\frac{-2\gamma.Cos\theta_2}{R_c}] = \rho gs \qquad \ldots (37)$$

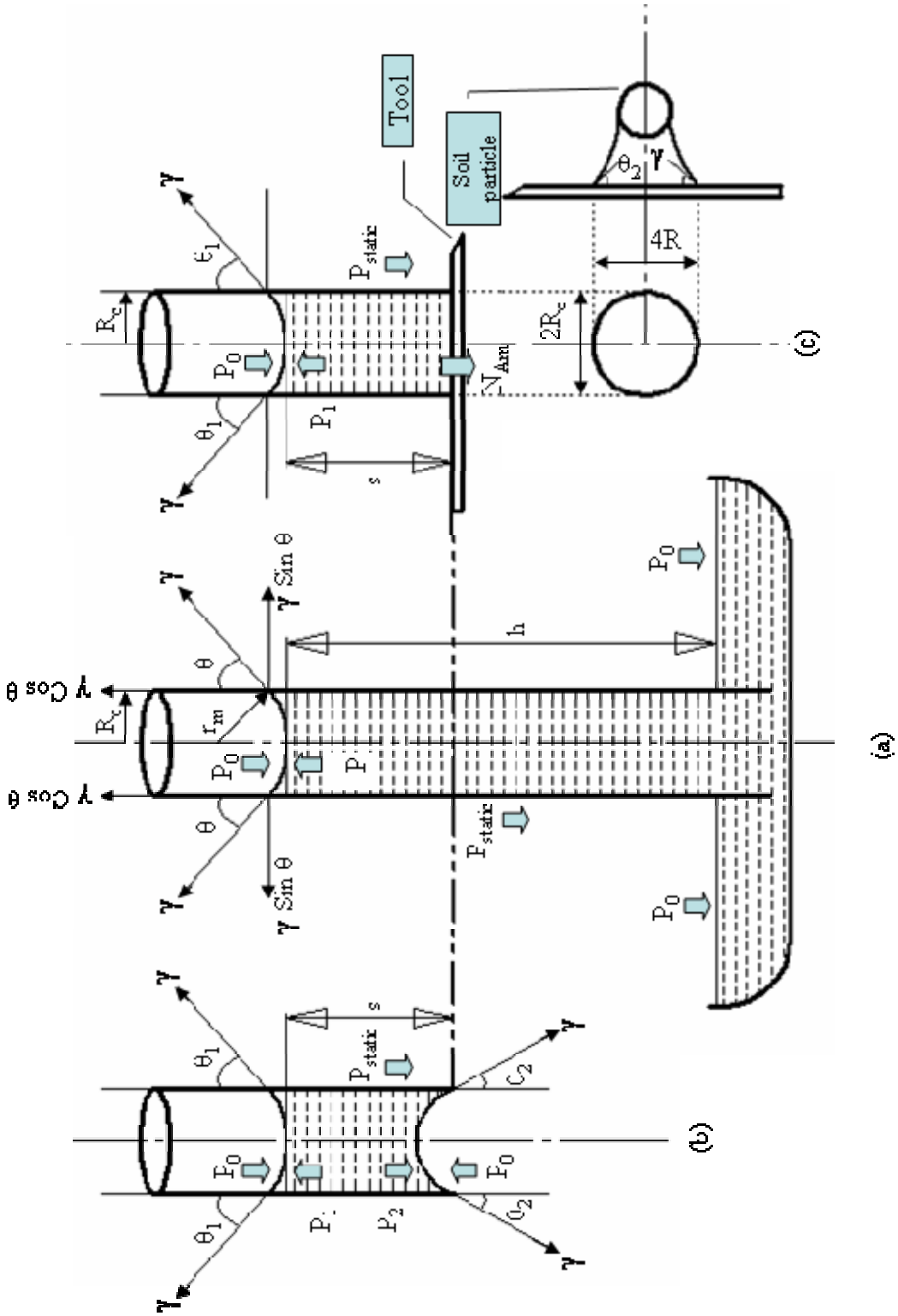

Figure 3. Force analysis for snipped capillary (a) capillary tube in liquid reservoir with a snipping plane (b) hypothetical snipped capillary section in air (c) snipped capillary section on tool surface and its equivalent soil particle (figure not to scale) (Modified and redrawn after Shi-qiao, 2004)

Rearranging the Eqn. (37) for *s*, we get,

$$s = \frac{2\gamma.(Cos\theta_2 - Cos\theta_1)}{\rho g R_c} \quad \ldots (38)$$

Eqn. (38) suggests a positive value of right hand side of equality sign for capillary rise (s > 0) and negative value for capillary depression (s < 0). Soil capillary pores undergo a capillary rise with water, thus contact angle at lower meniscus (θ_2) will always be smaller than the contact angle at upper meniscus (θ_1). It reveals that the lower meniscus have smaller curvature than that of the upper (Zheng, 2001).

Figure 3c describes a schematic of sheared capillary, which is cut by tool and closely touches its surface. The tool surface holds capillary water tightly under the action of normal adhesion of water meniscus (N_{Am}) on to it. The three agents act on the capillary water viz. the upward pulling pressure at upper meniscus (ΔP_1), the downward normal adhesion of meniscus by tool surface (N_{Am}) and the downward static pressure (P_{static}). At the partial equilibrium condition,

$$\Delta P_1 - \frac{N_{Am}}{\pi R_c^2} = \rho g s \quad \ldots (39)$$

But situations occur with shearing tools where interfacial water forms a film and completely seals capillary pores at their contact with tool surface. Under such circumstances the net ascending pressure difference ($\Delta P_1 - {N_{Am}}/{\pi R_c^2}$) will exceed the static pressure ($\rho g s$) (Shi-qiao, 2004) and a vacuum is created at the tool surface. Capillary adsorption of negative air pressure can be envisaged on the entire area (πR_c^2) encircled by the meniscus. In absence of the atmospheric pressure at the lower meniscus, ΔP_1 will be the Laplace pressure, thus,

$$\Delta P - \frac{N_{Am}}{\pi R_c^2} = \rho g s + \frac{N_{ca}}{\pi R_c^2} \quad \ldots (40)$$

Where,

N_{ca} = Normal adhesion force caused by capillary negative adsorption

MaFarlance and Tabor (1950) confirmed the importance of understanding surface tension to evaluate adhesion. Under saturated conditions water film contacts tool surface in circular vicinity whose diameter was empirically verified as *4R*, where *R* is the radius of spherical water asperity (Figure 3c).

A careful observation from Figure 3c reveals relation between the capillary tube radius (R_c) and radius of corresponding soil particle (R). The magnitude of N_{Am} can be expressed as,

$$N_{Am} = 2\,\pi R_c\,\gamma\,Cos\,\theta \quad \ldots (41)$$

From Eqns. (33) and (41), Eqn. (40) can be modified as,

$$\frac{2\gamma.Cos\theta}{R_c} - \frac{2\gamma.Cos\theta_2}{R_c} = \rho gs + \frac{N_{ca}}{\pi R_c^{\,2}} \quad \ldots (42)$$

Substituting value of static pressure from Eqn. (37),

$$\frac{2\gamma.Cos\theta}{R_c} - \frac{2\gamma.Cos\theta_2}{R_c} = \frac{2\gamma.Cos\theta_2}{R_c} - \frac{2\gamma.Cos\theta_1}{R_c} + \frac{N_{ca}}{\pi R_c^{\,2}} \quad \ldots (43)$$

Substituting $\theta_1 \rightarrow \theta$ and $\theta_2 \rightarrow 0^0$ for a snipped capillary with completely sealed lower meniscus, we get,

$$\frac{2\gamma.Cos\theta}{R_c} - \frac{2\gamma}{R_c} = \frac{2\gamma}{R_c} - \frac{2\gamma.Cos\theta}{R_c} + \frac{N_{ca}}{\pi R_c^{\,2}} \quad \ldots (44)$$

$$\frac{N_{ca}}{\pi R_c^{\,2}} = \frac{4\gamma.Cos\theta}{R_c} - \frac{4\gamma}{R_c} \quad \ldots (45)$$

Which gives,

$$N_{ca} = -4\pi\,\gamma\,R_c\,(1 - Cos\,\theta) \quad \ldots (46)$$

Negative value of Eqn. (46) reveals that it is a drawing vacuum, which is caused by capillary adsorption of negative pressure at tool surface. The theoretical maximum value of N_{ca} can be given as,

$$(N_{ca})_{max} = -\,8\,\pi\,\gamma\,R_c \quad \text{at } [\theta \rightarrow 180^0] \quad \ldots (47)$$

Furthermore, using Eqn. (32), Eqn. (42) can be modified for $\theta_2 \rightarrow 0^0$,

$$\rho gh - \frac{2\gamma}{R_c} = \rho gs + \frac{N_{ca}}{\pi R_c^{\,2}} \quad \ldots (48)$$

Which results,

$$N_{ca} = -[2\,\pi\,\gamma\,R_c - \rho g\,(h - s).\,\pi R_c^{\,2}] \quad \ldots (49)$$

2.3 Normal Friction Force (N_f)

The friction of ascending capillary contributes to the wet friction of interfacial water film meniscus and can be expressed as the normal wet friction of meniscus at the soil tool interface (N_{wfm}). Neglecting contribution of meniscus at individual soil particle, the total normal friction force (N_f) reasonably assumed to come from N_{wfm}.

Bowden & Tabor (1954) confirmed that the normal tensile force required to separate two solid surfaces depends on the speed of separation. Viscous resistance also plays an important

role in soil-tool adhesion, especially with continuous water film (Tong et al., 1999). Viscous resistance is developed due to the continuous water film at interface. Since the water film is not uniformly distributed, viscous resistance too is uneven and varies place to place. This uneven distribution results in pulling off some of the soil micro-sized particles and water molecules. Material properties of tool surface govern the amount of such soil particles been pulled off, which is different for different material (Tong et al., 1994). Some materials, including polyethylene, provides soil-free surface, while some shows soil-affinity. Viscous resistance largely depends on surface activity of the soil and tool surface and thickness of the interfacial water film. A system having higher activity of soil-tool with thinner water film would be having larger viscous resistance than that of with a system with smaller activity and thicker film. The system with high capillary attraction and high viscous resistance will obviously exhibit larger soil-tool adhesion (Tong et al., 1999).

When a liquid moves over the solid surface, a frictional force, which acts at right angle to the contact plane, opposes the motion (Schwartz et al., 1964). If N_{wfm} is the wet frictional force per unit length of the line of contact, acting normally and θ_A & θ_R are advancing and receding contact angles,

$$N_f = N_{wfm} = \frac{\gamma}{2}[\text{Cos } \theta_R - \text{Cos } \theta_A] \qquad \ldots (50)$$

Value of this N_{wfm} is independent of direction of travel i.e. N_{wfm} doesn't change when the direction of motion is reversed, which suggests that the solid-vapor and solid-liquid interfaces rapidly attain equilibrium.

The above analysis reveals that the total normal force (N) acting at the soil-tool interface comprises three major components – the normal gravitational force (N_G), the normal adhesion (N_A) and the normal friction (N_f). Normal gravitational force consists gravity of soil particles and the pores; normal adhesion contents the normal adhesion from bare soil particles, from water meniscus, from viscidity, and capillary negative adsorption; whereas, normal friction constitutes the normal wet friction of water meniscus. Using the magnitudes of aforementioned relations, N can be expressed as,

$$N = N_G + N_A + N_f \qquad \ldots (51)$$

$$N = [N_p + N_s] + [N_{As} + N_{Am} + N_{Av} + N_{ca}] + N_{wfm} \qquad \ldots (52)$$

$$N = \left[\sigma_s.S - (\sigma_s - \sigma_p).p.S\right] + \left[\left\{2\pi.W_A d_e^2 R.\left[\frac{1}{d_0^2} - \frac{1}{d_0(d_0+R)}\right]\right\}\right.$$
$$+ \left\{\frac{2\pi.R.\gamma}{\left[1+\frac{d_0}{b}\right]}(1+Cos\theta).\ Sin\ \theta\right\} + \left\{\left(\frac{3\pi.\eta.R^4}{4t}\right)\left(\frac{1}{h_1^2} - \frac{1}{h_2^2}\right)\right\}$$
$$\left. + \{4\pi\,\gamma\,R_c\,(1 - Cos\,\theta)\}\right] + \left[\frac{\gamma}{2}(Cos\,\theta_R - Cos\,\theta_A)\right] \qquad \ldots (53)$$

Alternatively,

$$N = [\sigma_s.S - (\sigma_s - \sigma_p).p.S] + [\{\frac{8}{3}\pi.R.E_A\left[\left(\frac{d_e}{d_0}\right)^2 - \frac{1}{4}\left(\frac{d_e}{d_0}\right)^8\right]\}$$
$$+ \{\pi R \gamma (1 + Cos \varphi) (3 - Cos \varphi)\} + \{\left(\frac{3\pi.\eta.R^4}{4t}\right)\left(\frac{1}{h_1^2} - \frac{1}{h_2^2}\right)\}$$
$$+ \{2 \pi \gamma R_c - \rho g (h - s). \pi R_c^2\}] + [\frac{\gamma}{2}(Cos \theta_R - Cos \theta_A)] \quad \ldots (54)$$

3. TANGENTIAL FORCES ACTING AT SOIL-TOOL INTERFACE

Tangential forces (τ) at the interface can be grouped under three components, viz. tangential friction, drag resistance and tangential adhesion.

3.1 Tangent Frictional Resistance (τ_f)

Neglecting friction generated by organic matter, impurities and the soil pores at the interface, the tangent frictional resistance (τ_f) can be approximately equal to the tangent resistance due to the dry friction of soil particles.

3.1.1 Tangent Resistance Due to Dry Friction of Soil Particles (τ_{dfs})

At very low water contents (water range – *a* in Table 1) with negligible adhesion between soil particles and tool surface, bare soil particles produce rubbing action against the surface. The dry friction, caused by the bare soil particles (τ_{dfs}), contributes to tangent frictional resistance and acts in the lateral tangential direction, opposite to the direction of soil travel over tool surface. If μ_{dfs} is the coefficient of dry friction of soil particles on tool surface (Liu, 1993),

$$\tau_f = \tau_{dfs} = \mu_{dfs} N_s \quad \ldots (55)$$

3.2 Drag Resistance (τ_{drag})

With increase in water content at the interface, free water is available to undergo a relative motion with moving tool. The backward dragging force acts tangentially on any liquid layer. The drag resistance (τ_{drag}) is mainly dominated by the tangential viscidity at the interface.

3.2.1 Drag Resistance Due to Tangential Viscidity (τ_{tv})

Newton showed that viscous force is directly proportional to the surface area (S) of the layer and velocity (v), and inversely proportional to its distance (x) from the stationary layer. If the coefficient of proportionality is η, which is the coefficient of viscosity, then,

$$\tau_{drag} = \tau_{tv} = -\eta S \frac{dv}{dx} \quad \ldots(56)$$

3.3 Tangential Adhesive Resistance (τ_A)

Tangential adhesive resistance comes from surface tension and water meniscus adhesion.

3.3.1 Tangential Adhesive Resistance Due to Surface Tension ($\tau_{tA\gamma}$)

Relative motion of soil particles with respect to the tool surface distorts associated meniscus. In the situation of pulling a water film over a tool-surface, meniscus obtains a distorted shape. Viewing from the front of the interface, the contact angle there (θ_f) will be larger than the static contact angle (θ); while the contact angle at the back (θ_b) will be smaller (Figure 4). Depending on the velocity of pull the values of distortion changes and so with the tangential adhesion force (F_t). With higher speeds and higher normal adhesion force, it is possible to witness θ_f as an obtuse angle and θ_b be zero (Hu et al., 2001). The horizontal component of θ_b, along the interface plane, resists the motion and as θ_b approaches zero, this component claims higher contribution (Shi-qiao, 2004). If l_t is the total accumulative length of surface tension (γ) relative to θ_f and θ_b, then the $\tau_{tA\gamma}$ can be expressed as,

$$\tau_{tA\gamma} = [\gamma_b \, Cos \, \theta_b - \gamma_f \, Cos \, \theta_f] \, l_t \quad \ldots (57)$$

where γ_b and γ_f are backside and frontside surface tension of liquid, respectively.

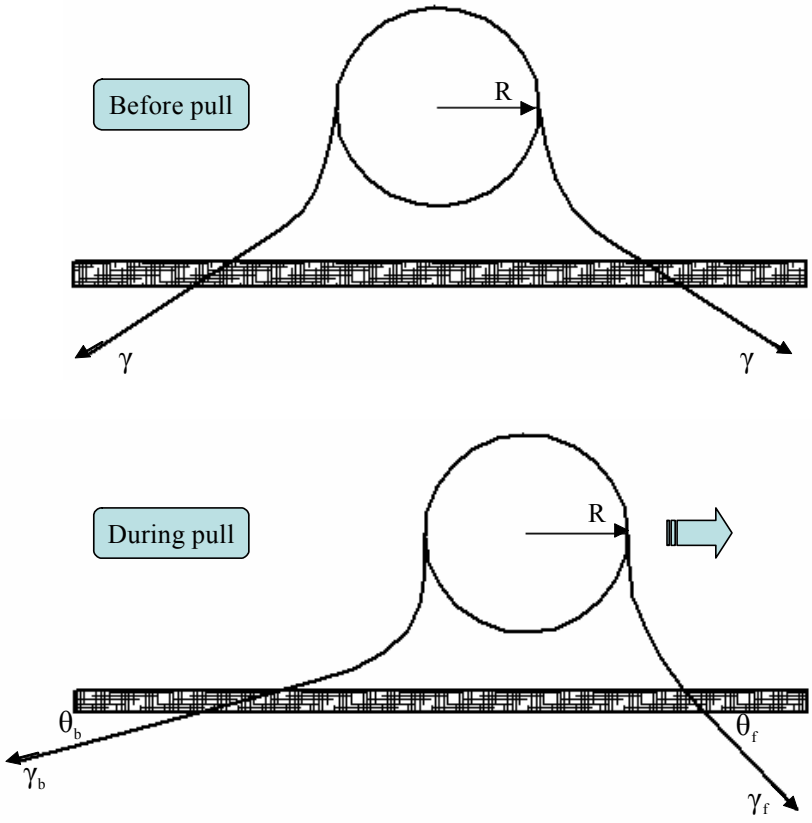

Figure 4. Meniscus deformation producing tangent adhesion during pull (figure not to scale)

For simplicity, it can be assumed that $\gamma_b = \gamma_f = \gamma$ (Zeng, 1995), thus

$$\tau_{tA\gamma} = \gamma\,[Cos\,\theta_b - Cos\,\theta_f]\,l_t \qquad \ldots (58)$$

3.3.2 Tangential Adhesive Resistance Due to Water Meniscus (τ_{tAm})

For the film-like water at the interface, water ring results in meniscus tensile force, whose magnitude is expressed by Eqn. (20). Component of F_{Am} in the direction parallel to interface would give tangential resistance due to water meniscus (τ_{tAm}),

$$\tau_{tAm} = F_{Am.}Cos\,\theta = \frac{2\pi.R.\gamma}{\left[1+\frac{d_0}{b}\right]}\left(1+Cos\,\theta\right).\,Cos\,\theta \qquad \ldots (59)$$

Thus from Eqns. (58 & 59), the total tangential adhesive resistance (τ_A) could be expressed as,

$$\tau_A = [\tau_{tA\gamma} + \tau_{tAm}] = \gamma\,[Cos\,\theta_b - Cos\,\theta_f]\,l_t + \frac{2\pi.R.\gamma}{\left[1+\frac{d_0}{b}\right]}\left(1+Cos\,\theta\right).\,Cos\,\theta \qquad \ldots (60)$$

Above analysis reveals that the total tangent force (τ) acting at the soil-tool interface comprises three major components – the tangent frictional resistance (τ_f), the drag resistance (τ_{drag}) and the tangent adhesive resistance (τ_A). Tangential frictional resistance consists dry friction of soil particles; drag resistance contents the tangential viscidity; whereas, tangent adhesive resistance constitutes the surface tension and water meniscus. Using the aforementioned relations, magnitude of τ can be expressed as,

$$\tau = \tau_f + \tau_{drag} + \tau_A \qquad \ldots (61)$$

$$\tau = \mu_{dfs} N_s + \eta\, S\, \frac{dv}{dx} + \gamma\,[Cos\,\theta_b - Cos\,\theta_f]\,l_t + \frac{2\pi.R.\gamma}{\left[1+\frac{d_0}{b}\right]}\left(1+Cos\,\theta\right).\,Cos\,\theta \qquad \ldots (62)$$

4. TOTAL MICROSCOPIC FORCES AT INTERFACE (F)

Practical difficulty and complicacy experienced by researchers (Shi-qiao, 2004) in demarcating adhesive and frictional forces at the soil-tool interface led a newer approach of grouping such forces into mutually perpendicular components – normal (N) and tangent (τ) to the interface. The total microscopic force at the interface (F), using equations Eqns. (51 & 61), can be expressed,

$$F = \sqrt{\left(N^2 + \tau^2\right)} \quad \ldots (63)$$

$$F = \sqrt{\left(N_G^2 + N_A^2 + N_f^2\right) + \left(\tau_f^2 + \tau_{drag}^2 + \tau_A^2\right)} \quad \ldots (64)$$

5. CONCLUSIONS

Microscopic interfacial forces at the soil-tool interface were reviewed and major forces were clubbed into two mutually perpendicular groups – normal and tangent to the interface. Water content plays an important role to alter relative strength of the each component. Other factors influencing microscopic forces include intrinsic properties of tool, surface conditions, tool material, physical and chemical composition of soil. Capillary suction or negative pressure is induced from the soil pores, is the main cause of normal adhesive resistance, while the contact area at soil-tool interface largely contributes to the tangent resistance.

Normal force acting at the interface comprises three primary components – normal gravity, normal adhesion and normal friction. Gravitational force is contributed by soil particles and soil water; normal adhesion comes from intermolecular attraction of bare soil particles, water meniscus, water film's viscidity and capillary negative adsorption; and normal friction is composed of wet friction of water meniscus.

Tangent resistance at the interface constitutes three components – tangential friction, drag and tangential adhesion. Tangent friction is mainly caused by dry friction of soil particles; drag resistance comes from tangential viscidity; and tangential adhesion is due to surface tension and water meniscus.

It can be predicted that the resistance reduction at the interface could be achieved by eliminating capillary negative pressure and lowering the physico-chemical adsorption at the soil-tool interface. Having closer insight to microscopic descriptors of forces at soil-tool interface would certainly allow efficient and energy-saving design of soil-engaging tools. Moreover, it may lead to appropriate design modifications of interacting surfaces. Experimental validation can be done by precise investigations to further explore microscopic phenomena at the soil-tool interface.

6. NOTATIONS USED

Subscripts

a	:	Adsorption
A	:	Adhesion
c	:	Capillary
d	:	Dry
e	:	Equilibrium
f	:	Friction
G	:	Gravitational
i	:	Individual
m	:	Meniscus
p	:	Soil pores (assumed to be filled with water with negligible air)

s	:	Soil particles
t	:	Tangent
v	:	Viscosity
w	:	Wet
γ	:	Surface tension

Symbols

$h\omega$	:	Lifishitz-Van der Waals constant, J
b	:	Vertical distance between soil particle surface to its lowest tip, m
d	:	Separation between parallel planes of soil particle and tool surface, m
d_0	:	Separation between the summit tip and tool surface, m
d_e	:	Equilibrium intermolecular distance (shortest possible distance), m
$E(d)$	:	Interaction energy per unit area of separation, J/m^2
E_A	:	Energy of adhesion, J/m^2
F	:	Total microscopic force at the interface, N
F_{Am}	:	Adhesion force of water meniscus, in the direction of surface tension, N
h	:	Height of capillary water, m
h_1, h_2	:	Separation between discs, m
l_t	:	Total accumulative length of surface tension, m
N	:	Total normal force at interface, N
N_A	:	Normal adhesive force, N
N_{Am}	:	Normal adhesion force caused by meniscus, N
N_{As}	:	Normal adhesion force caused by bare soil particles, N
N_{Av}	:	Normal adhesion force caused by water film due to viscosity, N
N_{ca}	:	Normal adhesion force caused by capillary negative adsorption, N
N_f	:	Normal friction, N
N_G	:	Total gravitational force normal to interface, N
N_p	:	Weight of water-filled soil pores (water filled) at interface, N
N_s	:	Weight of soil particles at interface, N
N_{wfm}	:	Normal wet friction of interfacial water film meniscus, per unit length of the line of contact, N
p	:	Percent of pore space at the soil-tool interface, % of total cross sectional area
P	:	Pressure inside liquid column near the meniscus, Pa
$P(d)$	:	Attraction pressure per unit area of separation, Pa
P_0	:	Atmospheric pressure, Pa
P_1, P_2	:	Pressure inside liquid column near the upper and lower meniscus, respectively, Pa
P_{AC}	:	Negative pressure existing at the liquid wedge at the level AC, Pa
P_{static}	:	Static pressure of water column at corresponding height, Pa
r	:	Curvature radius of meniscus, m
R	:	Radius of soil particle asperity, m
R_{AC}	:	Radius of curvature of the interface at point A, m
R_c	:	Radius of capillary tube, m
S	:	Total contacting area of soil-tool interface, m^2
s	:	Distance between the lowest point of upper meniscus and the shearing plane, m

S_i	:	Section area of individual soil pore, m^2
S_p	:	Total area of soil pores, m^2
S_s	:	Total contact area of soil particles, m^2
t	:	Time required to pull two parallel plates, s
v	:	Tool velocity, m/s
W_A	:	Work of adhesion, J
x	:	Distance of liquid layer from the tool surface, m
γ, γ_{LV}	:	Surface tension at liquid-vapor interface, N/m
γ_b, γ_f	:	Backside and frontside surface tension, respectively, N/m
γ_{SL}	:	Surface tension at solid-liquid interface, N/m
γ_{SV}	:	Surface tension at solid-vapor interface, N/m
η	:	Coefficient of dynamic viscosity, dyne-sec/cm^2 or poise
θ	:	Contact angle between meniscus and tool surface, degree
θ_1 , θ_2	:	Contact angles are upper and lower meniscus, respectively, degree
θ_A	:	Advancing contact angle, degree
θ_b	:	Contact angle at the back of meniscus, degree
θ_f	:	Contact angle at the front of meniscus, degree
θ_R	:	Receding contact angle, degree
μ_{dfs}	:	Coefficient of dry friction of soil
ρ , ρ_2	:	Density of liquid, kg/m^3
ρ_1	:	Density of solid soil particles, kg/m^3
ρ_3	:	Density of second fluid surrounding the whole system, kg/m^3
σ_p	:	Mean gravitational stress of soil pores, Pa
σ_s	:	Mean gravitational stress of soil particles, Pa
τ	:	Total tangential/sliding (lateral) resistance at interface, N
τ_A	:	Adhesive component of tangent resistance, N
τ_{dfs}	:	Tangent resistance from dry friction of soil particles, N
τ_{drag}	:	Drag component of tangent resistance (τ), N
τ_f	:	Frictional component of tangent resistance (τ), N
τ_{tAm}	:	Tangent resistance due to tangent adhesion of water meniscus, N
$\tau_{tA\gamma}$	:	Tangent resistance due to tangent adhesion of surface tension, N
τ_{tv}	:	Tangent resistance due to viscous forces, N
φ	:	Angle, with vertical, made by the radius with the point at which the liquid surface meets sphere, degree

7. REFERENCES

Akiyama, Y. and O. Yokoi. 1972. Study on soil adhesion, Part II. Theoretical analysis of adhesion mechanism at the saturating stage. *Journal of Japanese Soil Fertilizer Science*, 43(8):271-277 (In Japanese).

Bikerman, J. J. 1974. Capillary attraction and hysteresis of wetting. *Journal of Adhesion*, 6:331-336.

Bowden, F. P. and D. Tabor. 1954. *Friction and Lubrication of Solids*. Oxford Clarendon Press, London.

Chancellor, W. J. 1994. *Friction between soil and equipment materials – review*. ASAE Paper No. 94-1034.

Chen, B., Cong, Q. and L. Ren. 1996. Soil adhesion mechanism of chemical absorption. In: *Proceedings of the 12th International Conference of the ISTVS*, pp. 546-551.

Cong, Q., Ren, L., Chen, B. and F. Su. 1990. A study on adhesion reducing methods of terrain-machine. Transactions of the *Chinese Society of Agricultural Engineering*, 6(1):8-14 (In Chinese).

Fountaine, E. R. 1954. Investigations into the mechanism of soil adhesion. *Journal of Soil Science,* 5(2):251-263.

Gill, W. R. and G. E. Vanden Berg. 1968. *Soil Dynamics in Tillage and Traction*. Agricultural Handbook, No. 316. Agricultural Research Service. US Department of Agriculture.

Hu, Z., Chen, G. and Y. Du. 2001. *The Surface Interface of Materials*. East China University of Science and Technology Press, Shanghai, China (In Chinese).

Israelachvili, J. N., Fisher, L. R., Horn, R. G. and H. K. Christenson. 1982. Tribology Series 7: *Microscopic Aspects of Adhesion and Lubrication,* New York, pp. 55-66.

Jia, X. 2004. Theoretical analysis of the adhesion force of soil to solid materials. *Biosystems Engineering,* 87(4):489-493.

Liu, J. 1993. *The Theory of Material Abrasion and its Anti-abrasion Characteristics*. Tsinghua University Press, Beijing, China (In Chinese).

McFarlance, J. S. and D. Tabor. 1950. Adhesion of solids and the effect of surface films. In: Proceedings of the *Royal Society of London*, Series A: Mathematical and Physical Sciences, pp. 224-243.

Michael, A. M. (1998). *Irrigation: Theory and Practice.* Vikas Publishing House, New Delhi, India.

Oida, A. and M. Momozu. 2002. Simulation of soil behavior and reaction by machine part by means of DEM. Agricultural Engineering International: the CIGR Journal of Scientific Research and Development. Manuscript PM 01 004. Vol. IV. October, 2002.

Orr, F. M. and L. E. Scriven. 1975. Pendular rings between solids: Meniscus properties and capillary force. *Journal of Fluid Mechanics*, 67(4):123-142.

Oswal, M. C. 1994. *Soil Physics*. Oxford & IBH Publishing Co. Pvt. Ltd. New Delhi.

Princen, H. M. 1969. *The equilibrium shape of interfaces, drops, and bubbles: Rigid and deformable particles at interfaces.* In: Matijevic, E. (editor), Surface and Colloid Science, Vol. 2. Willey-Interscience, New York, pp. 1-84.

Qian, D. 1965. Study on the adhesion characteristics of the conventional mouldboard material – white iron against wet clay soil. Transaction of the *Chinese Society of Agricultural Machinery*, 8(2):145-150 (in Chinese).

Ren, L. Q., Tong, J., Li, J. Q., and B. C. Chen. 2001. Soil adhesion and biomimetics of soil-engaging components: A review. *Journal of Agricultural Engineering Research*, 79(3):239-263.

Schwartz, A. M., Rader, C. A. and E. Huey. 1964. *Resistance to Flow in Capillary Systems of Positive Contact Angle*. In Gould, R. F. (Editor) Contact Angle, Wettability, and Adhesion. Advances in Chemistry Series. American Chemical Society, Washington, D. C., pp. 250-267.

Shi-qiao, D. 2004. *The mechanism of reducing soil adhesion and the design of bionic plow*. Ph.D. thesis, Jilin University (Unpublished) (In Chinese).

Shi-qiao, D., Lu-quan, R., Yan. L., and H. Zhi-wu. 2005. Tangent resistance of soil on moldboard and the mechanism of resistance reduction of bionic moldboard. *Journal of Bionics Engineering,* 2(1):33-46.

Tong, J., Ren, L. Q., Chen, B., and A. R. Qaisrani. 1994. Characteristics of adhesion between soil and solid surfaces. *Journal of Terramechanics*, 31(2):93-105.

Tong, J., Ren., L. Q., Yan, J. L., Ma, Y. H., and B. C. Chen. 1999. Adhesion and abrasion of several materials against soil. *Agricultural Engineering Journal,* 8(1):1-22.

Wu, S. 1982. *Polymer Interface and Adhesion*. Marcel Dekker, New York, pp. 54-62.

Xiong, S. 2001. *Basic Agrology.* China Agricultural University Press, Beijing, pp. 96-131 (In Chinese).

Zeng, D. 1995. *The Dynamics of Mechanical-Edaphic System*. Agricultural Handbook. Beijing Science and Technology Press, Beijing, China (In Chinese).

Zhang, R. and J. Li. 2004. Simulation on mechanical behavior of cohesive soil by Distinct Element Method. In: *Proceedings of the 7th Asia-Pacific Conference on the ISTVS*, Changchun, China, September 14-16, 2004, pp. 154-161.

Zhang, R. and J. Li. 2006. Simulation on mechanical behavior of cohesive soil by Distinct Element Method. *Journal of Terramechanics*, 43:303-316.

Zhang, R., Li, J. and S. Xu. 2004a. Simulation of force on nonsmooth bulldozing plate by Distinct Element Method. In: *Proceedings of 2004 CIGR International Conference*, Beijing, China, October 11-14, 2004, 30-160D: III-166.

Zheng, S. 2001. Capillary phenomena and contact angles. *Journal of Gansu Advance Normal College*, 6(2):29-31.